EX-SITU TIME-LAPSE X-RAY CT STUDY OF 3D MICRO-STRUCTURAL FATIGUE DAMAGE EVOLUTION IN UNI-DIRECTIONAL COMPOSITES

Kristine M. Jespersen*[1], Ying Wang[3], Jens Zangenberg[2], Tristan Lowe[3], Philip J. Withers[3], Lars P. Mikkelsen[1]

[1]Department of Wind Energy, Section of Composites and Materials Mechanics, Technical University of Denmark, Risø Campus, 4000 Roskilde, Denmark (Email: kmun@dtu.dk*)
[2]LM Wind Power Blades, Composite Mechanics, Jupitervej 6, 6000 Kolding, Denmark
[3]Manchester X-ray Imaging Facility, School of Materials, University of Manchester, Manchester M13 9PL, United Kingdom

Keywords: Micro-tomography, Glass fibre reinforced polymer, Damage progression, Off-axis cracks, Fibre fractures

Abstract
In this study, the progress of damage under tension-tension fatigue of a uni-directional (UD) glass fibre composite made from a non-crimp fabric is studied using transilluminated white light imaging (TWLI) and X-ray computed tomography (CT). TWLI images are automatically captured throughout the fatigue test, and at two damage levels the test is stopped and the sample is examined by X-ray computed tomography. From the TWLI observations it is apparent that part of the measured initial stiffness drop might be caused by edge effects rather than off-axis cracking. Some of the off-axis cracks are seen to initiate already after the first cycle, whereas some grow gradually and others appear suddenly during cycling. The off-axis cracks are observed to saturate after a few thousand cycles. The UD fibre fracture damage in the region observed by X-ray CT is probably already saturated at the first interruption point, as no significant change is seen between the two X-ray images. However, the study indicates how TWLI can be used as an initial indicator to locate damage regions at an early stage for the future ex-situ X-ray CT experiments.

1. Introduction

Fibre composites are increasingly being used to replace metals in many weight sensitive industries such as the aerospace, automotive and wind energy sector. Compared to airplanes and vehicles, wind turbine blades experience repeated loading to a much higher extent [1]. Variations in the wind causes the blades to repeatedly bend flap-wise in the direction of the tower. In addition, the blade rotation causes the gravitational load of the blades to repeatedly change direction resulting in repeated edge-wise bending of the blades. During the 20-30 years of life of a wind turbine blade the total number of load cycles sum up to the range of $10^8 - 10^9$ cycles [1]. As a result, fatigue is one of the limiting factors when designing a large wind turbine blade [2]. Because of the specific load conditions, uni-directional (UD) fibre composites made from non-crimp fabrics (NCFs) are commonly used to carry the primary bending loads in the blade, and the fatigue damage mechanisms for this material are not well understood. In order to improve the fatigue resistance and/or establish more reliable methods to predict the fatigue life-time, it is necessary to understand the fatigue damage mechanisms on a microstructural level. This is the focus of the current study.

Excerpt from ISBN 978-3-00-053387-7

1.1. Fatigue damage progression in fibre composites

Fatigue damage in fibre composites has received much focus in literature, however fatigue damage progression in fibre composites is complex. Several damage mechanisms such as fibre/matrix debonding, matrix cracking, and fibre fractures occur and interact with each other [3]. Furthermore, the damage mechanisms are dependent on many things such as the lay-up, materials, fibre/matrix interface, loading and more. For cross-ply and other angle-ply laminates, tension fatigue damage is known to initiate in the off-axis layers as tunnelling cracks [4, 5]. These cracks then result in more serious damage such as fibre fractures and interlaminar delaminations.

The UD NCF composites used for wind turbine blades generally include thin layers of off-axis fibres, which to some extent makes them similar to "extreme" angle-ply composites with thin off-axis layers compared to the UD. However, in NCFs the fibres are gathered in bundles and the off-axis fibre bundles generally have isolated points where they cross over each other. It has been observed in previous studies [6, 7] that the UD fibre damage during tension fatigue appear locally rather than uniformly distributed across the material. Furthermore, the locations of the UD fibre damage regions are closely related to these cross-over points for the thin off-axis fibre bundles. This leads to quite complex damage mechanisms, which are difficult to monitor and predict.

1.2. Non-destructive damage observation

In-situ (or ex-situ) X-ray CT makes it possible for the progress of internal damage to be observed non-destructively. So far, in-situ X-ray CT experiments of damage progression in fibre composites have generally been performed using synchrotron radiation X-ray CT [8–11] because of the relatively short scan time. However, due to limited access time, fatigue damage progression experiments such as those by Garcea et al. [10, 11] only consider a few thousand load cycles. Recent advances in laboratory X-ray CT has resulted in image quality competitive to synchrotron CT, but at longer scan times. Using laboratory X-ray CT makes it easier to perform longer duration start-stop studies, which would not be possible using synchrotrons due to the limited access. Only a few studies have considered damage in fibre composites using laboratory X-ray CT (e.g. [12–14]) and in particular studies considering individual fibre fractures and the progress of damage over time have been limited to date.

When it comes to damage observation, a limitation of X-ray CT is that it relies on differences in density to get contrast in the image. This means that if cracks are closed, they are likely not to be visible in the image. This is particularly challenging in relation to matrix and interface cracks, although a number of strategies have been applied to improve this [15]. For glass fibre composites transilluminated white light imaging (TWLI) as also used in [4, 5] can be used to monitor cracks in 2D. In the current study, TWLI is used in combination with X-ray CT to observe the damage progression over time in a UD NCF glass fibre composite. The study demonstrates the advantage of combining these observation techniques and highlights promising future aspects.

2. Composite material system and specimen geometry

The considered composite was a UD glass fibre/polyester resin composite made from a non-crimp fabric. The fabric was made from parallel UD fibre bundles, which were stitched to a thin layer of off-axis ($\pm 80°$) supporting backing bundles (the same fabric used in [6, 7]). The composite was made by stacking two layers of fabric with the backing sides facing each other in the centre ($[0/b]_s$), and then impregnating them with resin using vacuum assisted resin transfer moulding (VARTM) infusion. End tabs were glued on to a plate of the composite and small rectangular specimens were cut out for fatigue testing. The specimen length was 117mm with a gauge section of 40mm. The tabs were tapered over a length of

Excerpt from ISBN 978-3-00-053387-7

10mm towards the gauge section to decrease stress concentrations in the laminate.

3. Experimental methods

Fig. 1a shows a sketch of the typical shape of the stiffness degradation response for the composite material outlined in Section 2 during tension-tension fatigue. Within the initial few thousand cycles, the stiffness drops by a few percent as indicated by region I in Fig. 1. Thereafter, the stiffness degrades stably for a high number of cycles, which is shown as region II. Finally, as marked by region III, the stiffness starts to decrease drastically followed by final failure. As also indicated in Fig. 1a, the idea is to use TWLI to monitor the initiation and growth of transverse cracks (region I) and then use X-ray CT to monitor the stable stiffness degradation (region II). In previous studies [6, 7], UD fibre fractures have been reported during region II, and X-ray CT is used to observe these failures, as they cannot be seen by the TWLI camera.

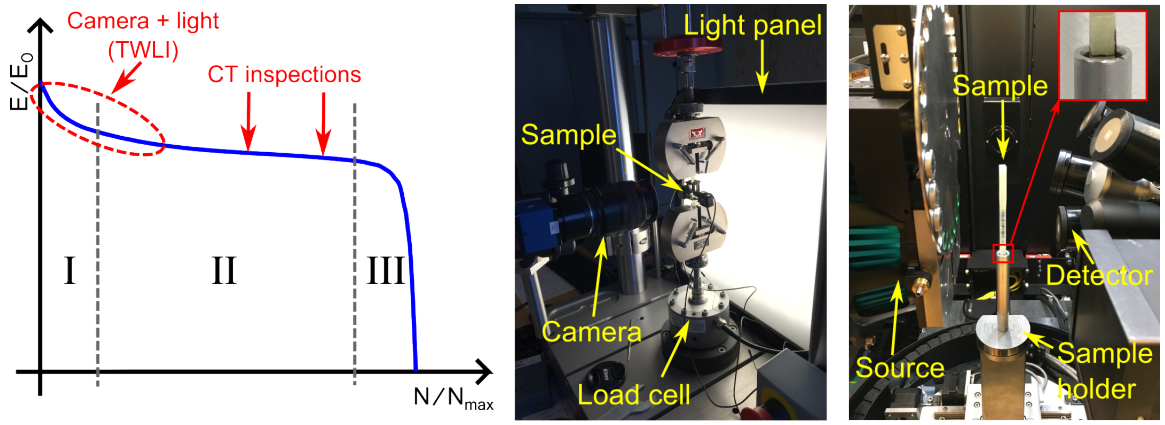

a) Typical stiffness degradation and examination idea

b) Fatigue test

c) X-ray CT

Figure 1. a) shows the typical shape of the stiffness degradation response for the considered material, b) the fatigue test including the TWLI setup, and c) the sample mounted in the X-ray CT scanner.

3.1. Fatigue testing and off-axis crack monitoring

The fatigue tests were carried out on an Instron Electropuls E3000 (max 3 kN) at 0.6% strain in load control with a sinusoidal waveform. The load range based on the desired strain of the test was determined from two initially performed static tensile tests to obtain the initial Young's modulus. The test was carried out with a stress-ratio of R=0.1, a test frequency of 10Hz, and the strain was monitored using one extensometer having a gauge length of 25mm and a maximum deflection of 2.5mm. The test was interrupted at two points in the loading history for X-ray examination.

A camera of type SVS-Vistek SVCam EVO8050 GigE with a Nikon AF Micro Nikkor 60mm 1:2.8D lens was mounted on the fatigue test setup and a light panel was placed behind the test specimen to highlight cracks as shown in Fig. 1b. The camera was connected to a trigger box ensuring automatic image acquisition during the test. As crack initiation and growth appear at a faster pace in the beginning of the test, images were acquired at the peak of every load cycle for the first 100 cycles, after which the number of images acquired was decreased to keep the amount of data down without compromising the results. The aim was to acquire 100 images per fatigue cycle decade.

Excerpt from ISBN 978-3-00-053387-7

3.2. X-ray computed tomography

The X-ray CT experiments were carried out on a laboratory type Zeiss Xradia Versa 520 scanner. Two sets of scan settings were used as shown in Table 1. All scans were performed using a detector with 4x optical magnification and a pixel depth of 16 bit. The pixels on the detector were binned down with a factor of 2 (binning 2). The sample was mounted in a specially made cylindrical aluminum holder as shown in Fig. 1c. It was made from a solid cylindrical piece, and a hole corresponding to the longest diagonal on the sample cross section was drilled with a depth of 30 mm. To be able to repeatedly mount the sample in approximately the same way, both the sample and the holder were marked with a pen as also seen in Fig. 1c.

Table 1. Overview of x-ray CT scan settings

Scan name	Source to sample distance (mm)	Detector to sample distance (mm)	Exposure time (s)	No. of projections -	Accelerating voltage (keV)	Pixel size (μm)
MR	24	30	2	3201	70	3.13
HR	24	55	7	4601	70	2.05

Since the UD fibre fractures are local phenomena it can be difficult to locate a region with damage if choosing a location arbitrarily. To locate a damage region in the sample, the photos of the off-axis cracks were evaluated and an initial scan region was located where a medium resolution (MR in Table 1) scan was carried out to confirm the locations of fibre fractures. Based on the observed damage regions in this scan, a re-centered high resolution (HR in Table 1) scan was performed. The re-centering was done to get the damage as central as possible in the field of view (FoV) and was done using the "Scout-and-scan" principle suggested by Zeiss.

4. Results and discussion

Fig. 2 shows the measured stiffness degradation during the fatigue test. The data for the full test are shown in Fig. 2a. Several points of interest have been marked, and point E and F indicates where the fatigue test was interrupted for CT examination. The slight drop in measured stiffness after the interruption is likely to be because two extensometers (instead of one as for the first part) were used to measure the strain for the final 50,000 cycles. However, it is seen that the difference is minimal and that the trend is unaffected. A zoom on the initial stiffness degradation part is shown in Fig. 2b. A steep drop of around 1% in stiffness is observed between 0 cycles and point A, which is more clearly seen in Fig. 2c.

Camera images were acquired during the full test and the corresponding camera images of a few of the points of interest marked in Fig. 2 are shown in Fig. 3. In Fig. 3 it is seen that a few off-axis cracks have appeared after the initial E-modulus test (corresponding to two cycles). A significant increase in the number of off-axis cracks is seen from point 0 to point A (480 cycles), which is probably the origin of the steep initial stiffness drop of around 1% seen in Fig. 2c. The steep linear decrease in stiffness seen between point A and B in Fig. 2b is likely to be caused by a gradual increase in the number of off-axis cracks as seen by the difference between point A and B in Fig. 3. There is only a small difference observed in the number of off-axis cracks between point B and C. However, edge damage is seen to initiate around point B, and it is possible that the stiffness drop between point B and C is more related

Excerpt from ISBN 978-3-00-053387-7

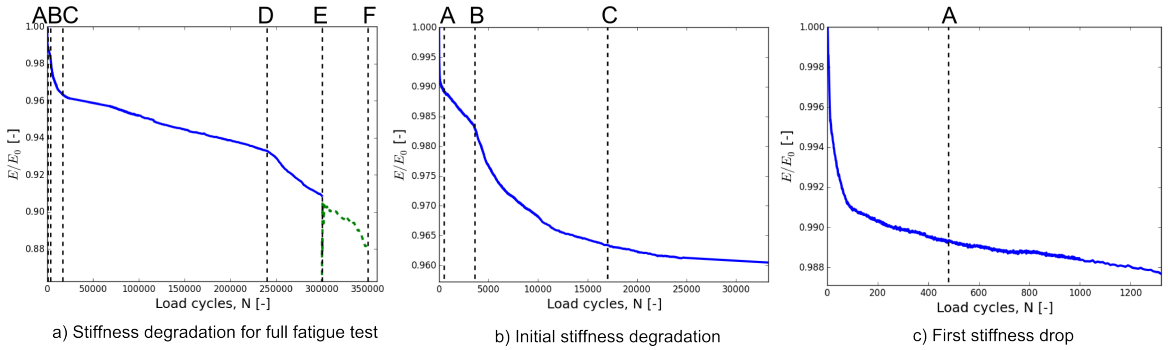

Figure 2. Normalised stiffness degradation for the fatigue test. a) shows the full test, b) a zoom on the initial stiffness degradation region, and c) the first steep stiffness drop. The marked points of interest; A, B, C, D, E, and F correspond to 480, 3600, 17000, 240000, 300000, 350000 cycles, respectively. Point E and F represent the points at which the test was interrupted for X-ray CT.

to edge effects than to actual damage mechanisms of the material. Between point C and D the stiffness degrades stably. At point C, what looks like local delaminations (probably between the backing bundle layers) in the loading direction starts to gradually grow (visible at point D in Fig. 3). After point D the inclination of the stiffness degradation becomes steeper. Perhaps surprisingly, there is almost no difference in the photos taken at point D and E.

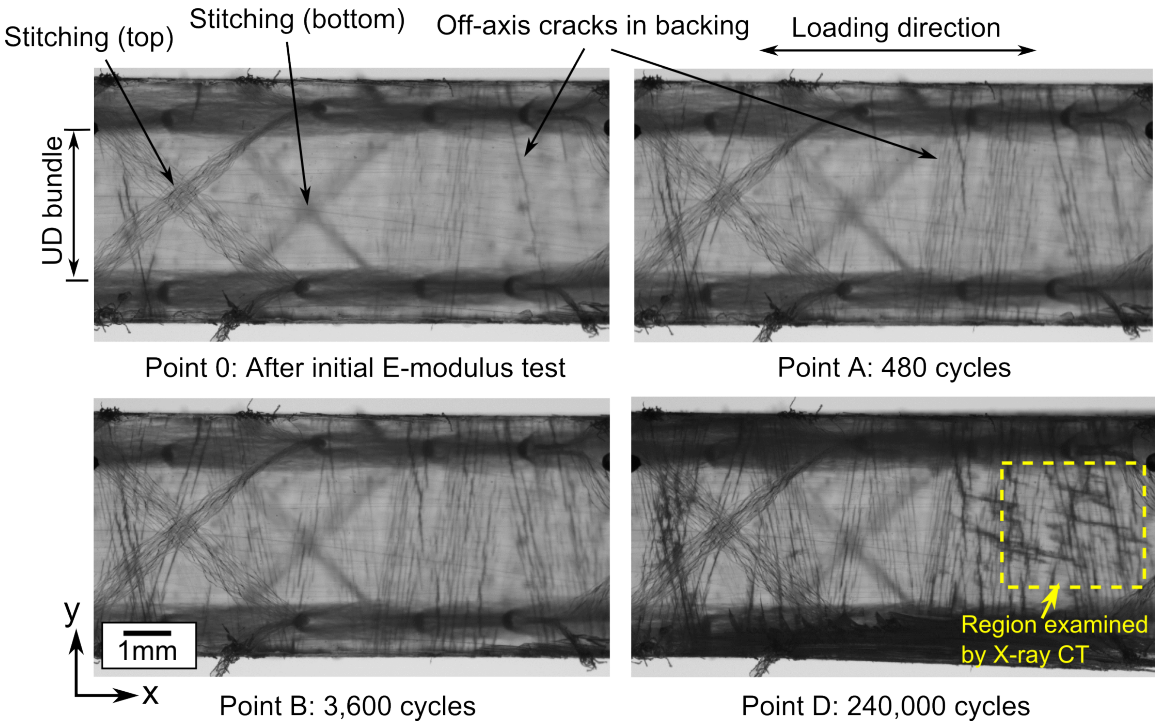

Figure 3. TWLI camera images acquired during fatigue testing. The region imaged by CT in Fig. 4 is shown.

The fatigue test was interrupted at point E, and the sample was examined by X-ray CT in the region where the photos indicated that UD fibre fractures were likely to be present (See point D in Fig. 3). After X-ray CT scanning of the sample, it was fatigued for an additional 50,000 cycles as seen by the dashed green curve between point E and F in Fig. 2a, and scanned once again. Fig. 4 shows a virtual slice of the 3D X-ray CT data in approximately the same location for the two scans. No significant

Excerpt from ISBN 978-3-00-053387-7

change in damage is observed although there are a few additional UD fibre fractures (see arrow in Fig. 4). Nevertheless, it may be possible that the two slices are not exactly in the same location or the slice angle is slightly different. Therefore, an automatic quantification method for fibre fractures is necessary for proper comparison, and this is therefore currently a topic of ongoing work. As no or little change in damage was observed, it is likely that the damage region was already saturated at the point of the first scan, and that damage regions in other locations were growing instead. Therefore it is necessary to find and follow damage regions at a point earlier in the fatigue life in order to follow the damage propagation. This can be quite challenging as the FoV is small and the damage regions are isolated local regions. However, the photos of the transverse cracks along with initial overview CT scans can be used as guidance to choose the scan location to follow over time. This is currently ongoing work.

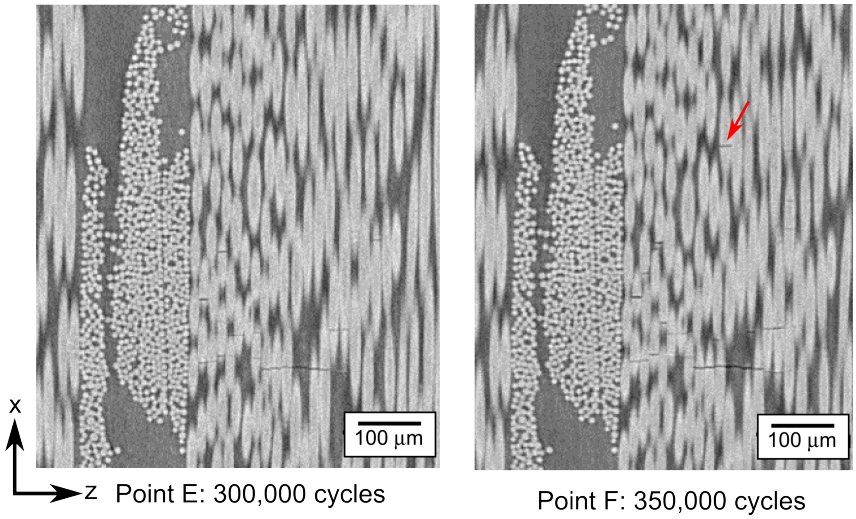

Figure 4. Virtual 2D x-z slice extracted from 3D X-ray CT data for point E and F. No particular change in damage is observed.

Even though the fibre failures are seen quite clearly in Fig. 4, it is not possible to see any matrix cracks in the backing bundles. That is despite knowing from the results in Fig. 3, that they are present. As discussed previously in [7], this is a matter of insufficient resolution (~2-3μm) since the opening of these cracks is small. Here, it is important to remember that the camera photos were taken at the point of maximum load during the fatigue test. Fig. 5 shows the camera images of point D where Fig. 5a is the loaded sample and Fig. 5b is when the load is removed. It is evident that most of the matrix cracks almost close completely when the load is removed, which explains why they are difficult to see using X-ray CT on the unloaded specimen. Therefore it is of interest to also apply tension during scanning, as watching the off-axis cracks in 3D would provide additional useful information about the damage mechanisms as proposed by [15].

5. Conclusion

In this study the tension-tension fatigue damage progression of a uni-directional glass fibre composite made from a non-crimp fabric was studied. The initiation and growth of off-axis cracks were studied by transilluminated white light imaging and the UD fibre fractures were examined by X-ray CT. The measured stiffness degradation was compared to the corresponding camera images and discussed. No change in size of the fibre fracture region was seen by X-ray CT, however it is believed that the observed region was already saturated. The cause of the stiffness degradation between the two interruption points is believed to be the growth of UD fibre fracture regions at other locations in the sample that are not yet saturated. However, this will have to be confirmed. In the future, a damage region will be located at an

Excerpt from ISBN 978-3-00-053387-7

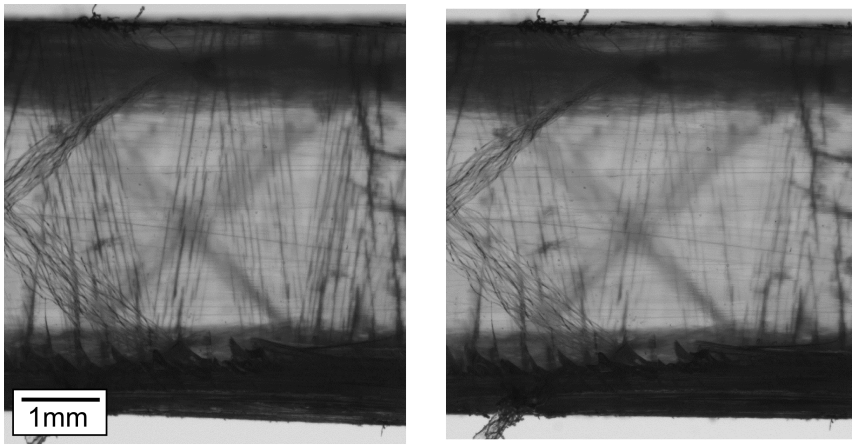

Figure 5. Camera images after 300,000 cycles where a) shows the loaded and b) unloaded sample.

earlier stage with guidance from observed transverse cracks and a quick overview X-ray CT scan, and the growth of the UD fibre fracture region monitored by X-ray CT.

Acknowledgments

The author would like to acknowledge the assistance provided by the Manchester X-ray Imaging Facility, which was funded in part by the EPSRC (grants EP/F007906/1, EP/F001452/1 and EP/I02249X/1). Financial support from CINEMA: "the allianCe for ImagiNg of Energy MAterials", DSF-grant no. 1305-00032B under "The Danish Council for Strategic Research" is gratefully acknowledged. Additionally, we would like to thank LM Wind Power for manufacturing of test specimens.

References

[1] R. P. L. Nijssen. Fatigue life prediction and strength degradation of wind turbine rotor blade composites. *PhD Thesis, Delt University of Technology*, 2006.

[2] R. P. L. Nijssen and P. Brøndsted. Fatigue as a design driver for composite wind turbine blades. *Advances in Wind Turbine Blade Design and Materials*, pages 175–209, 2013.

[3] W. W. Stinchcomb and K. L. Reifsnider. Fatigue damage mechanisms in composites materials: a review. *Fracture Mechanisms, Proceedings of an ASTM-NBS-NSF symposium, ASTM STP 675*, pages 762–787, 1979.

[4] M. Quaresimin, P. A. Carraro, L. P. Mikkelsen, N. Lucato, L. Vivian, P. Brøndsted, B. F. Sørensen, J. Varna, and R. Talreja. Damage evolution under cyclic multiaxial stress state: A comparative analysis between glass/epoxy laminates and tubes. *Composites: Part B*, 61:282–290, 2014.

[5] J. A. Glud, J. M. Dulieu-Barton, O. T. Thomsen, and L. C. T. Overgaard. Automated counting of off-axis tunnelling cracks using digital image processing. *Composites Science and Technology*, 125:80–89, 2016.

[6] J. Zangenberg, P. Brøndsted, and J. W. Gillespie Jr. Fatigue damage propagation in unidirectional glass fibre reinforced composites made of a non-crimp fabric. *Journal of Composite Materials*, 48(22):2711–2727, 2014.

Excerpt from ISBN 978-3-00-053387-7

[7] K. M. Jespersen, T. Lowe, P. J. Withers, J. Zangenberg, and L. P. Mikkelsen. Fatigue damage assessment of uni-directional glass/polyester composite using x-ray computed tomography. *Composites Science and Technology*, 2016. (Submitted).

[8] P. Wright, A. Moffat, I. Sinclair, and S. M. Spearing. High resolution tomographic imaging and modelling of notch tip damage in a laminated composite. *Composites Science and Technology*, 70(10):1444–1452, 2010.

[9] A. E. Scott, M. Mavrigirdati, P. Wright, I. Sinclair, and S. M. Spearing. In situ fibre fracture measurement in carbon-epoxy laminates using high resolution computed tomography. *Composites Science and Technology*, 71(12):1471–1477, 2011.

[10] S. C. Garcea, M. Macrigirdato, A. E. Scott, I. Sinclair, and S. M. Spearing. Fatigue micromechanism characterisation in carbon fibre reinforced polymers using synchrotron radiation computed tomography. *Composites Science and Technology*, 99(88):23–30, 2014.

[11] S. C. Garcea, I. Sinclair, and S. M. Spearing. In situ synchrotron tomographic evaluation of the effect of toughening strategies on fatigue micromechanisms in carbon fibre reinforced polymers. *Composites Science and Technology*, 109:32–39, 2015.

[12] P. J. Schilling, B. P. R. Karedla, A. K. Tatiparthi, M. A. Verges, and P. D. Herrington. X-ray computed microtomography of internal damage in fiber reinforced polymer matrix composites. *Composites Science and Technology*, 65(14):2071–2078, 2005.

[13] F. Sket, R. Seltzer, J. M. Molina-Aldareguía, C. Gonzalez, and J. LLorca. Determination of damage micromechanisms and fracture resistance of glass fiber/epoxy cross-ply laminate by means of X-ray computed microtomography. *Composites Science and Technology*, 72(2):350–359, 2012.

[14] B. Yu, R. Blanc, C. Soutis, and Withers P. J. Evolution of damage during the fatigue of 3D woven glass-fibre reinforced composites subjected to tension–tension loading observed by time-lapse X-ray tomography. *Composites: Part A*, 82:279–290, 2016.

[15] B. Yu, R. S. Bradley, C. Soutis, and P. J. Withers. A comparison of different approaches for imaging cracks in composites by x-ray microtomography. *Philosophical Transactions of the Royal Society A*, 2016. http://dx.doi.org/10.1098/rsta.2016.0037, In press.

Excerpt from ISBN 978-3-00-053387-7